Fuel 160 (2015) 424–433

Contents lists available at ScienceDirect

Fuel

journal homepage: www.elsevier.com/locate/fuel

Fuel temperature influence on spray and combustion characteristics in a constant volume combustion chamber (CVCC) under simulated engine operating conditions

Joonsik Hwang [a], Youngsoo Park [a], Choongsik Bae [a,*], Jinwoo Lee [b], Soonchan Pyo [c]

[a] Department of Mechanical Engineering, Korea Advanced Institute of Science and Technology, Republic of Korea
[b] Ulsan College, Republic of Korea
[c] Hyundai Motors Co., Republic of Korea

HIGHLIGHTS

- Cold diesel fuel exhibited deteriorated vaporization characteristics.
- Flame luminosity with cold diesel fuel was lower than warm diesel fuel.
- Cold diesel fuel showed lower in-chamber pressure and longer ignition delay.
- Ambient condition had more dominant effect than fuel temperature on combustion.

ARTICLE INFO

Article history:
Received 9 June 2015
Received in revised form 31 July 2015
Accepted 4 August 2015
Available online 8 August 2015

Keywords:
Fuel temperature
Macroscopic spray
Combustion
Constant volume combustion chamber (CVCC)
Cold start

ABSTRACT

High amount of unburned hydrocarbon emission and combustion instability are serious problems in diesel engines during cold starting. In order to solve these troubles, the effects of fuel temperature on spray and combustion should be understood. In this study, macroscopic spray and combustion experiments were carried out over a wide range of fuel temperatures from 243 to 313 K. The tests were performed under simulated low temperature cold start condition. In-chamber pressure analysis and high speed imaging were combined in a constant-volume combustion chamber (CVCC). The diesel fuel was injected into the CVCC under simulated engine operating conditions with an injection pressure of 35 MPa. The cold diesel fuel showed a longer liquid penetration length and a narrower spray angle in macroscopic spray imaging. The reasons for the deteriorated spray characteristics were revealed to be the attenuation of the fuel evaporation and ambient air entrainment. In combustion imaging, partial misfires of the diesel spray were detected under cold start condition. On the other hand, all of spray plumes were successfully ignited under hot start condition. The peaks of in-chamber pressure and flame luminosity were decreased with cold fuel because of the poor air–fuel mixture preparation during the ignition delay period.

1. Introduction

Although many technical improvements have been made to diesel engines, a serious problem still remains for starting at low ambient temperatures. In cold conditions, the low ambient air temperature results in a low peak compression temperature. The cylinder head and the engine block absorb most of the heat during the compression stroke, so the peak pressure also decreases [1]. In addition to the thermal conditions of the engine, the deterioration of fuel properties affects the mixture preparation during ignition delay period. Such conditions cause misfires with a high amount of hydrocarbon (HC), carbon monoxide (CO) and smoke emissions by poor air fuel mixing process [2]. However, in this situation, the cold start problem is getting worse because current emission regulations force the compression ratio of diesel engines to be further reduced [3–6]. To improve the cold startability, air temperature within the combustion chamber should be raised by using ignition aids, such as intake heaters or glow plugs [7,8]. Current automobile diesel engines require these aids for the ambient temperatures below 262 K [9].

With respect to the cold startability, most researches have focused on improving ignition by using various combustion strategies, such as applications of high pressure injection, multiple

* Corresponding author. Tel.: +82 42 350 3063; fax: +82 42 350 5023.
E-mail address: csbae@kaist.ac.kr (C. Bae).

http://dx.doi.org/10.1016/j.fuel.2015.08.004
0016-2361/

Nomenclature and Abbreviations

d_o	nozzle hole diameter (m)
I	intensity of a pixel
$\dot{m}_a$	entrained gas mass flow rate (kg/s)
$\dot{m}_f$	injected fuel mass flow rate (kg/s)
N	pixel number
$P_{w\ fuel\ spray}$	chamber pressure with fuel spray (MPa)
$P_{w/o\ fuel\ spray}$	chamber pressure without fuel spray (MPa)
Re	Reynolds number
ρ_{amb}	ambient density (kg/m^3)
ρ_{fuel}	fuel density (kg/m^3)
T_{amb}	ambient temperature (K)
T_f	fuel temperature (K)
u_{eff}	effective velocity at the exit of the orifice (m/s)
$\frac{du}{dy}$	the derivative of the velocity (1/s)
V	mean injection flow velocity (m/s)
x	axial distance from the orifice (m)
μ	the dynamic viscosity (kg/m s)
τ_{yx}	shear stress in the fluid (N/m^2)
θ	spreading angle of the spray (Radian)
bTDC	before top dead center
CAD	crank angle degree
CO	carbon monoxide
CVCC	constant-volume combustion chamber
HC	hydrocarbon
LOL	flame lift of length
NO_x	nitrogen oxides
PM	particulate matters

injection and exhaust gas recirculation (EGR). Chartier et al. studied the effect of injection strategies on the cold start performance in an optical direct injection diesel engine at a very low ambient temperature down to 244 K [10]. They found that fuel evaporation was limited at a low temperature but the engine performance could be improved by using three pilot injections. Zhong et al. also investigated the impact of split injection on cold startability in a diesel engine [11]. In this research, 4-cylinder diesel engine was tested under ambient temperature of 273 K, 264 K and 254 K. The combustion and emission characteristics were compared between single and multiple injection cases. From the result, it was confirmed that split-main injection strategies could improve the cold startability by shortened cranking period and lowered engine speed overshoot. At the same time it reduced the injected fuel mass and unburned HC emissions by almost 50% during the cranking period. In terms of the spray experiments, Payri et al. examined internal nozzle flow and the macroscopic spray characteristics according to the temperature of the fuel [12]. They showed that the Reynolds number decreased as a result of the increased viscosity of the cold fuel. This flow characteristic resulted in poor atomization with a narrower spray angle and a shorter vapor penetration length. Research on the spray characteristics of the biodiesel fuel according to various fuel and ambient temperatures were conducted in a constant volume chamber [13]. The results indicated that the evaporation of the fuel was suppressed as the fuel temperature decreased from 360 to 300 K. These are presented in lengthened liquid penetration and a decreased vapor fuel mass.

In spite of these efforts, a comprehensive understanding of the spray and combustion characteristics of diesel fuel under various fuel temperature conditions has not yet been carried out. Most previous studies have concentrated on the engine performance and emission characteristics according to the atmospheric conditions. Therefore, this study presents visualizations of the macroscopic spray and combustion under wide range of fuel temperatures in a constant volume combustion chamber. In contrast with previous researches, the experiments were performed not only with different diesel fuel temperature but also under simulated engine operating conditions. To simulate cold and hot engine start conditions, different pre-ignition processes were carried out by adjusting reactant mixture. The diesel fuel was injected using a common-rail system with a temperature range from 243 to 313 K. The in-chamber pressure analyses, including a rise in pressure and the derivative of the in-chamber pressure were performed with high speed imaging.

2. Experimental setup and condition

2.1. Experimental equipment and test procedure

Fig. 1 shows a schematic diagram of the fuel injection system. The fuel tank was designed to control the fuel temperature within the range from 243 to 333 K by operating a refrigeration cycle and an electric heater. The coolant was circulated through cooling fins which are installed inside the fuel tank. On the other hand, the fuel temperature was also possible to be increased by electric heater which is located around the fuel tank. The precise fuel temperature control within ±0.1 K was available by proportional integral

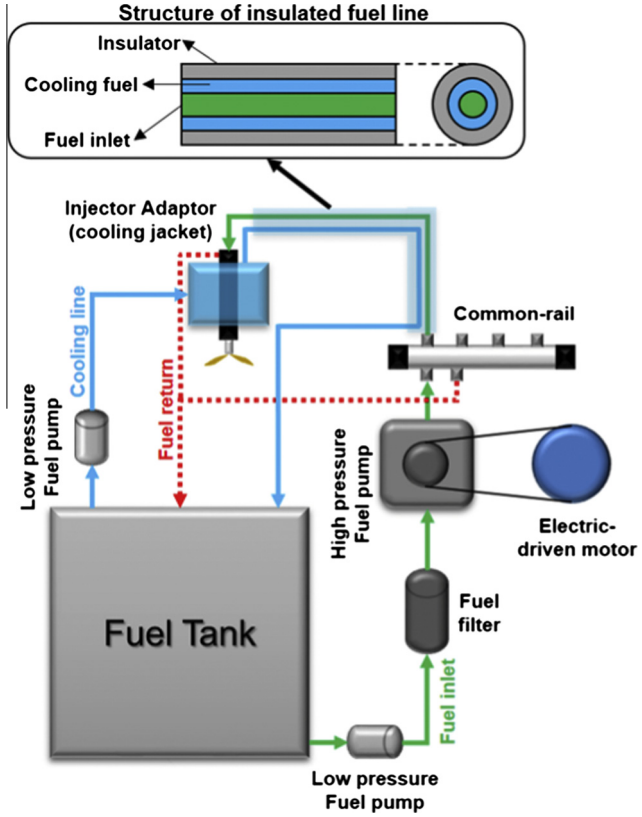

Fig. 1. Schematic diagram of fuel injection system.

Table 1
(a) Specifications of tested injector (b) Fuel properties of diesel fuel.

Item	Level
(a)	
Number of hole	7
Hydraulic flow rate (cm^3/30 s @ 10 MPa)	340
Hole diameter (μm)	124
Hole length (μm)	750
Included angle (°)	156
f-Factor	1.5

Item	Level	Analytic method
(b)		
Cetane number	51.9	ASTM D4737
Density (kg/m^3 @ 288 K)	815.6	ASTM D1298
Viscosity (mm^2/s @ 303 K)	2.4	ASTM D445
Pour point (K)	238	ASTM D5950
Cloud point (K)	262	ASTM D2500

derivative (PID) control based on the thermocouple signal. All of the return lines from the equipment were connected to hot reservoir to prevent temperature rise in the fuel tank. A common-rail injection system, including a high pressure fuel pump driven by an electric motor, was utilized for the fuel injection. The fuel was injected by using a seven-hole solenoid diesel injector, and the detailed specifications of the injector are depicted in Table 1(a). To maintain the fuel at a target temperature in the injector and the rail-to-injector fuel tube, the fuel was also circulated through the injector adaptor and the outer passage of rail-to-injector tube by using an additional low pressure fuel pump. The fuel injection pressure and the energizing time were controlled using a common-rail engine controller (Zenobalti, ZB-9013). The injector tip temperature was monitored during the experiments. The fuel properties are listed in Table 1(b). The tested fuel had pour point of 238 K so it was possible to lower the fuel temperature to 243 K without any waxing behavior.

Fig. 2 shows a schematic diagram of the CVCC system with the chamber that used to investigate the macroscopic spray and combustion characteristic. The CVCC has five 96 mm diameter quartz windows. The high pressure and high temperature ambient condition of a diesel engine was simulated by conducting pre-ignition before the fuel injection. Four gases (acetylene; C_2H_2, hydrogen; H_2, oxygen; O_2 and nitrogen; N_2) were mixed in a pre-mixing chamber, and then supplied to the CVCC through the intake valve. The chamber body was maintained at 473 K by using an electric heater to ensure the complete combustion of the pre-mixture. Two spark plugs were used to ignite the pre-mixture completely. The ratios of the combustion products, such as oxygen and carbon dioxide, were controlled by adjusting the composition of the reactant. The evaporating spray imaging was performed under a 0% oxygen concentration to prevent the fuel from igniting. On the other hand, a visualization of the combustion was conducted under a 21% oxygen concentration to mimic the atmospheric air. The chamber pressure was acquired using a piezo-electric pressure transducer (Kistler, 6141B type) with an acquisition frequency of 100 kHz. When the chamber pressure reached the target value during the cool down process, the fuel was injected by an injection signal. The overall pressure trace from pre-ignition to spray combustion can be shown in Fig. 3. The result of pre-ignition is presented by dotted line in the figure. The in-chamber temperature was calculated based on the acquired in-chamber pressure. The fuel was injected at the target pressure and temperature by adjusting the injection delay from start of pre-ignition. The injected fuel was ignited by high in-chamber pressure and temperature ambient condition. The pressure rise by injected fuel combustion can be seen in the solid line. The in-chamber pressure rise and the variation rate in the pressure were calculated through the following equations:

$$\Delta P = P_{w\ fuel\ spray} - P_{w/o\ fuel\ spray} \tag{1}$$

$$P' = \frac{d(\Delta P)}{dt} \tag{2}$$

where $P_{w\ fuel\ spray}$ is the in-chamber pressure with fuel spray, $P_{w/o\ fuel\ spray}$ is the in-chamber pressure without fuel spray (pre-combustion only), and t is the time.

It is difficult to make identical pre-combustions for each spray test. Therefore, the repeatability of pre-ignition was examined. The 5 times of repeated pre-ignition were performed under initial pressure of 0.1 MPa. From the test, standard deviation of maximum pressure and the timing were calculated as 0.0157 and 0.0238 respectively. This implies that the variation in the pre-combustion could be ignored.

A high-speed digital video camera (Photron, FASTCAM SA1.1) equipped with a prime lens (Nikkor, 60 mm f/2.8D) was used to capture images of the evaporating spray and combustion processes. The high speed camera trigger signal was synchronized to the fuel injection signal. The shutter speed of the high-speed camera was set to 20,000 frames per second (fps) for the spray test and 8200 fps for the combustion experiment, respectively. Mie-scattering method was adopted to capture liquid-phase fuel using a high intensity discharge lamp (HID Fire, HF-8500, 85W power). From the spray imaging, three images were averaged to estimate the liquid tip penetration length and the spray angle. This procedure was repeated for each nozzle hole. To measure the liquid penetration length and the spray angle, the spray boundary was determined by selecting a threshold value for the intensity. The liquid penetration length was defined as the distance between the nozzle-tip to the farthest axial location of the spray boundary. The spray angle was measured at the middle of the liquid penetration length. From the combustion imaging, maximum and minimum values of the normalized flame luminosity were respectively set to '1' and '0' for each pixel. The equation for the normalized flame luminosity is given as follows:

$$\bar{I} = \frac{\sum_i \sum_j I_{i,j}}{N} \tag{3}$$

where $I_{i,j}$ is the flame intensity at pixel position (i,j) and N is the pixel number.

2.2. Experimental condition

The simulated experimental conditions were divided into cold start and hot start cases. The engine motoring pressure, in-cylinder temperature and density were calculated for each case using the WAVE (RICARDO.co) software. The simulation was conducted based on a diesel engine which has a compression ratio of 17.3. The engine coolant temperature was assumed to be of 243 K for a cold start condition and 353 K for the hot start. The diesel fuel was injected into the CVCC at a specific moment after pre-ignition which corresponds to an injection timing of 15 crank angle degree (CAD) before the top dead center (bTDC) for the spray test and 0 CAD bTDC for the combustion experiment. The injection pressure was of 35 MPa, and the energizing time was 1450 μs. The reason for this set value is that the normal injection pressure for real diesel engine during cranking period is 30–40 MPa. The details of the experimental conditions are shown in Table 2. Before the experiment, the density and the viscosity of the tested fuel were measured to investigate the effect of the fuel temperature on its properties. Fig. 4 shows variations in the fuel density and kinematic viscosity according to the fuel temperature. The properties were measured by volume measurements and by using

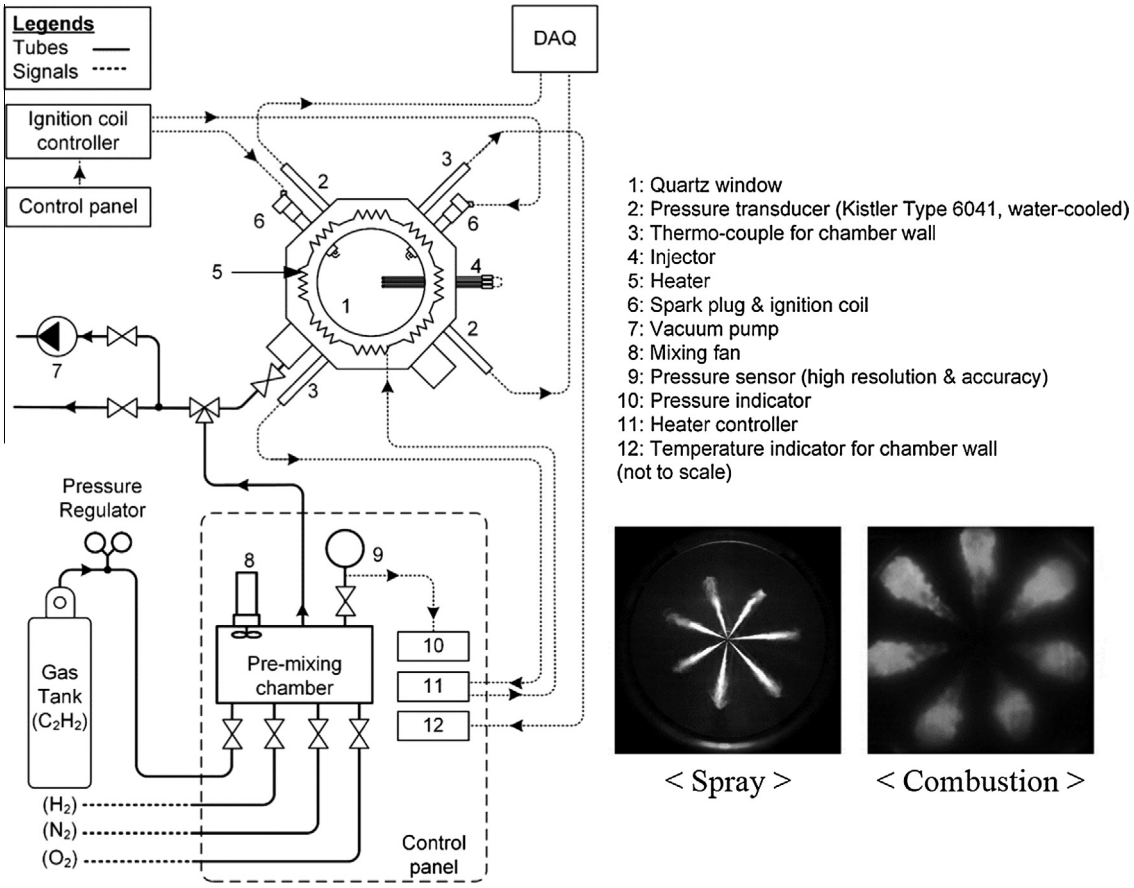

Fig. 2. Schematic diagram of constant volume combustion chamber system.

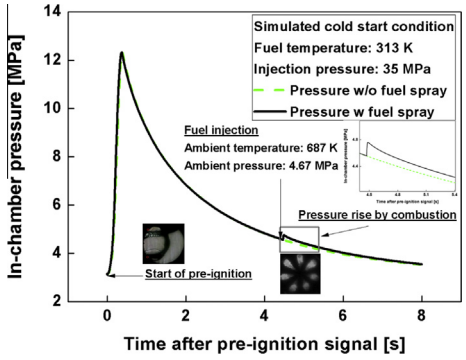

Fig. 3. Typical pressure trace from pre-ignition to spray combustion.

Table 2
Experimental conditions.

Parameter	Macroscopic spray	Combustion
Injection pressure (MPa)	35	
Energizing time (μs)	1450	
Oxygen concentration after pre-ignition (%)	0	21
Fuel temperature (K)	243, 258, 273, 283, 313	243, 273, 313
Simulated engine condition	Cold start	Cold start (C)/ Hot start (H)
Simulated injection timing in engine (CAD bTDC)	15	0
Ambient temperature (K)	626	687 (C)/961 (H)
Ambient pressure (MPa)	3.2	4.67 (C)/4.71 (H)
Ambient density (kg/m^3)	17.5	23.2 (C)/16.7 (H)

a viscometer, respectively. As the fuel temperature decreased from 313 to 243 K, the fuel density increased by 6%, and the kinematic viscosity increased approximately 12 times. The effect of the kinematic viscosity in response to the changes in fuel temperature can therefore be considered to be more dominant on the flow characteristics in the nozzle than density [12]. Meanwhile, the surface tension of diesel fuel is known to be increased linearly as fuel temperature decreased [14].

3. Results and discussion

3.1. Macroscopic spray characteristics under evaporating condition

Fig. 5 shows the sequential spray development of the diesel fuel at an injection pressure of 35 MPa with fuel temperatures of 243, 273 and 313 K. The images were obtained under a cold start condition. The time after start of energizing (ASOE) was defined as the duration from the injection signal. The part of injector tip was enlarged to examine the fuel injection event. From the figure, it was confirmed that the cold fuel was seen to have a longer injection delay. The small spray plume can be seen with warm fuel at 350 μs. On the other hand, the injector tip was clean with cold fuel. This behavior is strongly related to fuel viscosity. The injection delay of the high viscosity fuel was also detected by injection rate in previous research [12]. Common fluids follow Newtonian behavior under normal conditions. The Newton's law of viscosity for one-dimensional flow is given by following equation [15].

$$\tau_{yx} = \mu \frac{du}{dy} \tag{4}$$

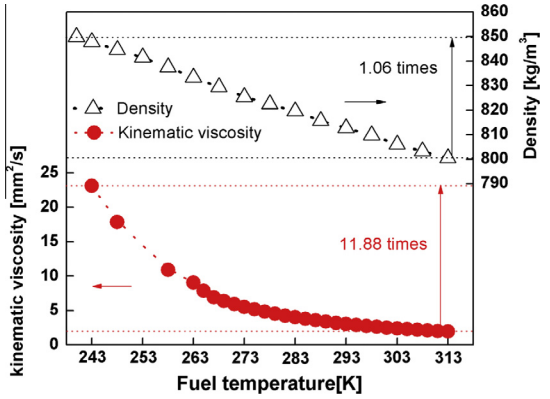

Fig. 4. Density and viscosity of diesel fuel according to fuel temperature [25].

where τ_{yx} is the shear stress in the fluid, μ the dynamic viscosity, and du/dy the derivative of the velocity component parallel to the shear direction, relative to the displacement in the perpendicular direction. The experimental conditions, such as injector configuration, injection signal and injection pressure were kept identical during the test. In this situation, the derivative of the velocity component with the cold fuel became smaller than that of the warm fuel due to higher dynamic viscosity. It can therefore be deduced that the derivative of the velocity component with fuel at 313 K is approximately 12 times larger than the fuel at 243 K. The high viscosity of the cold fuel slowed down the needle movement and decreased the flow performance of the injector. For this reason, additional control logic should be applied to adjust fuel injection timing in real vehicle application during the cold start condition. In terms of spray morphology, the spray boundary with warm fuel was became more dim than cold fuel due to enhanced atomization and vaporization characteristics.

Fig. 6 compares the liquid penetration length and the spray angle according to the fuel temperature. As shown in the figure, cold diesel was observed to have a relatively longer liquid penetration length and a narrower spray angle than warm diesel fuel. The Reynolds number (Re) was calculated in order to distinguish the flow characteristics of fuel spray since this number can be considered as a criteria to assess the atomization of the fuel spray. Re is the ratio of the inertia to the viscosity, as shown in the following equation [16]:

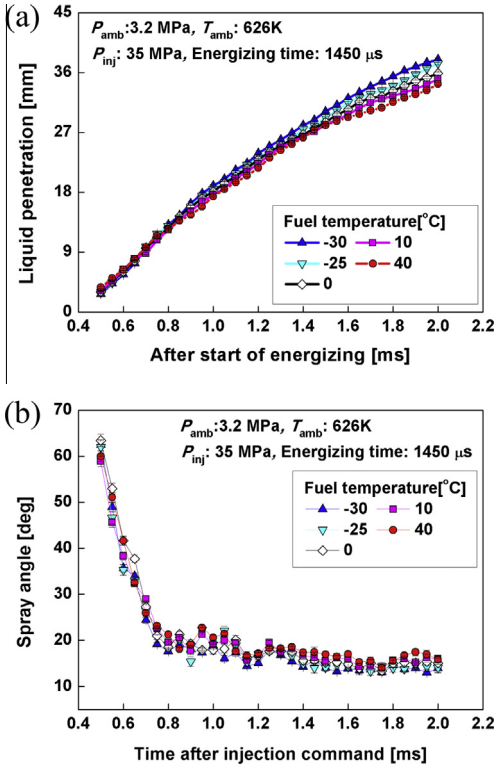

Fig. 6. Comparison of (a) liquid penetration tip length and (b) spray angle according to fuel temperature under cold start condition [20].

$$Re = (\rho_{fuel} V d_o)/\mu = (V d_o)/\nu \tag{5}$$

$$V = \sqrt{\frac{2\Delta P}{\rho_{fuel}}} \tag{6}$$

where ρ_{fuel} is the fuel density, V is the mean injection flow velocity, d_o is the nozzle hole diameter, μ is the dynamic viscosity, ν is the kinematic viscosity, and P is the pressure difference across the nozzle. The turbulent level of the internal nozzle flow is intensified as the Reynolds number increased. This turbulence can promote the separation of the boundary layer and the diffusion of the spray

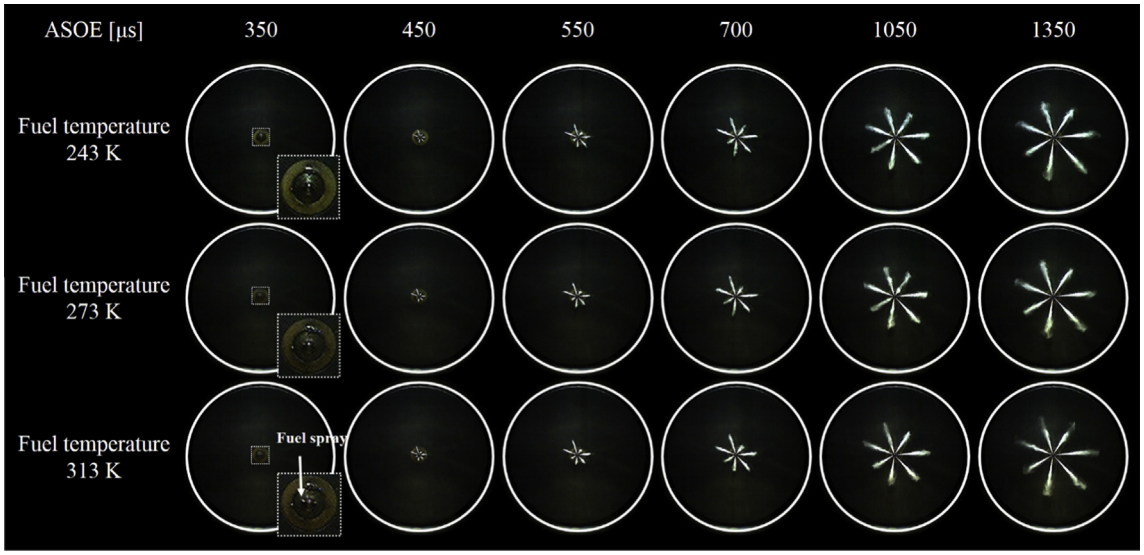

Fig. 5. Macroscopic spray according to fuel temperature under cold start condition (P_{inj}: 35 MPa, Energizing time: 1450 μs).

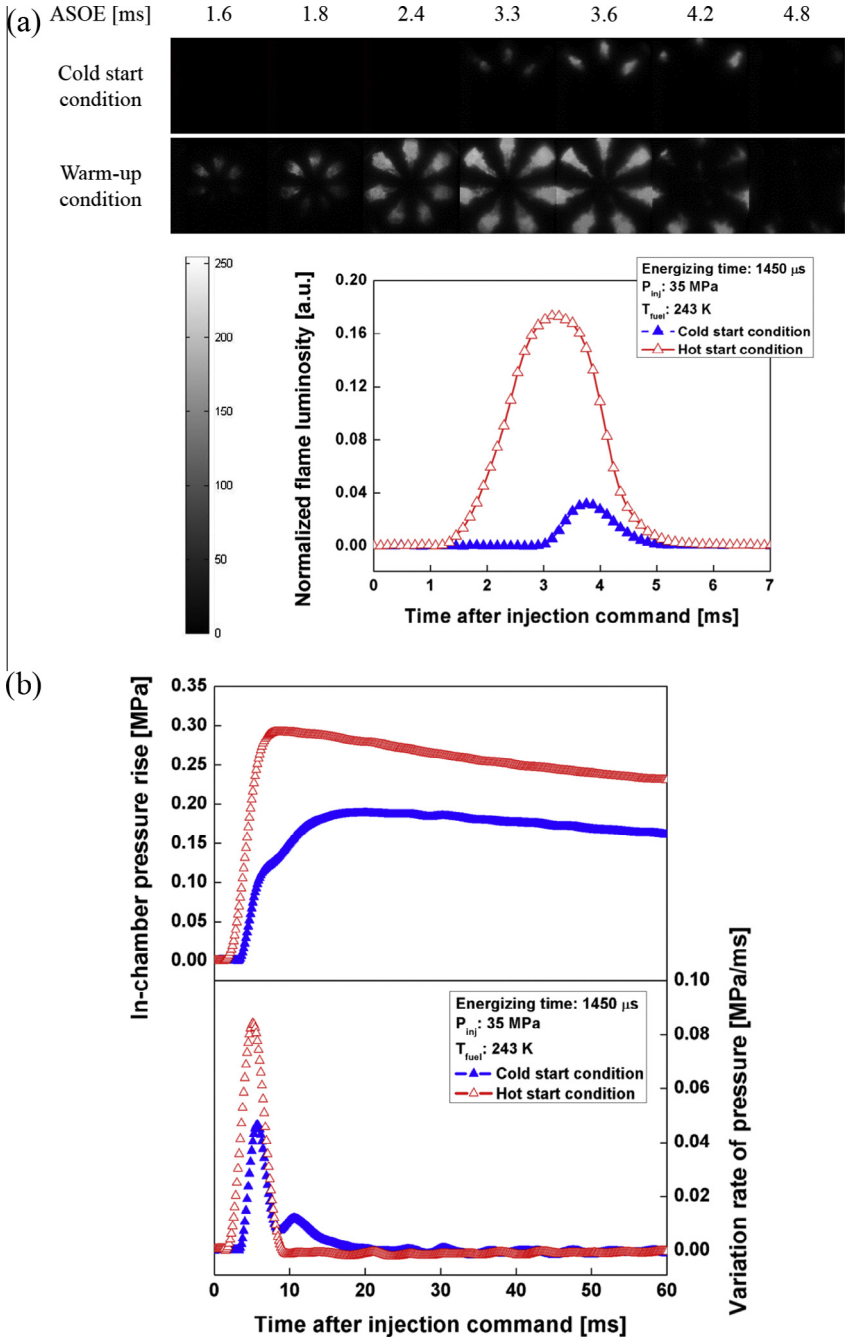

Fig. 7. (a) Normalized flame luminosity, (b) in-chamber pressure rise, and variation of pressure according to atmospheric conditions.

along the radial direction. *Re* was calculated to be of 1470, 6213, and 17,924 for 243, 273, and 313 K at an injection pressure of 35 MPa. The *Re* of the 243 K fuel was roughly 1/12 that of the 313 K fuel due to its higher viscosity. As a result, cold fuel had a narrower spray angle than diesel because of the more stable spray structure. The ratio of the entrained ambient gas to fuel by mass has been reported to be represented by the following equation [17], which shows that the value is inversely proportional to the fuel density.

$$\frac{\dot{m}_a}{\dot{m}_f} \propto \sqrt{\frac{\rho_a}{\rho_f}} \cdot \frac{x}{d_o} \cdot \tan\left(\frac{\theta}{2}\right) \tag{7}$$

where $\dot{m}_a$ is the total entrained gas mass flow rate, $\dot{m}_f$ is the injected fuel mass flow rate, ρ_a is the ambient gas density, ρ_f is the fuel density, d_o is the orifice diameter, x is the axial distance from the orifice, and θ is the spreading angle of the spray. The ambient gas density, the orifice diameter and the axial distance from the orifice are identical. Therefore, the equation can be simplified as a function of the fuel density and the spray angle. The calculated ratio of the entrained gas to the fuel by mass, $\frac{\dot{m}_{a/f,xK}}{\dot{m}_{a/f,313K}}$, was calculated to be of 0.82 for fuel at 243 K and 0.9 for fuel at 273 K. These results indicate that the higher density of the cold fuel demands an increase in the mixing length. The fuel spray has also been significantly affected through the viscosity and surface tension. The higher viscosity and surface tension of the cold fuel resisted the formation of surface waves, ligaments and droplets [18]. It was found that the breakup point of fuel spray shifted closer to the nozzle as the surface tension decreased. The size of fuel droplets also got decreased with low

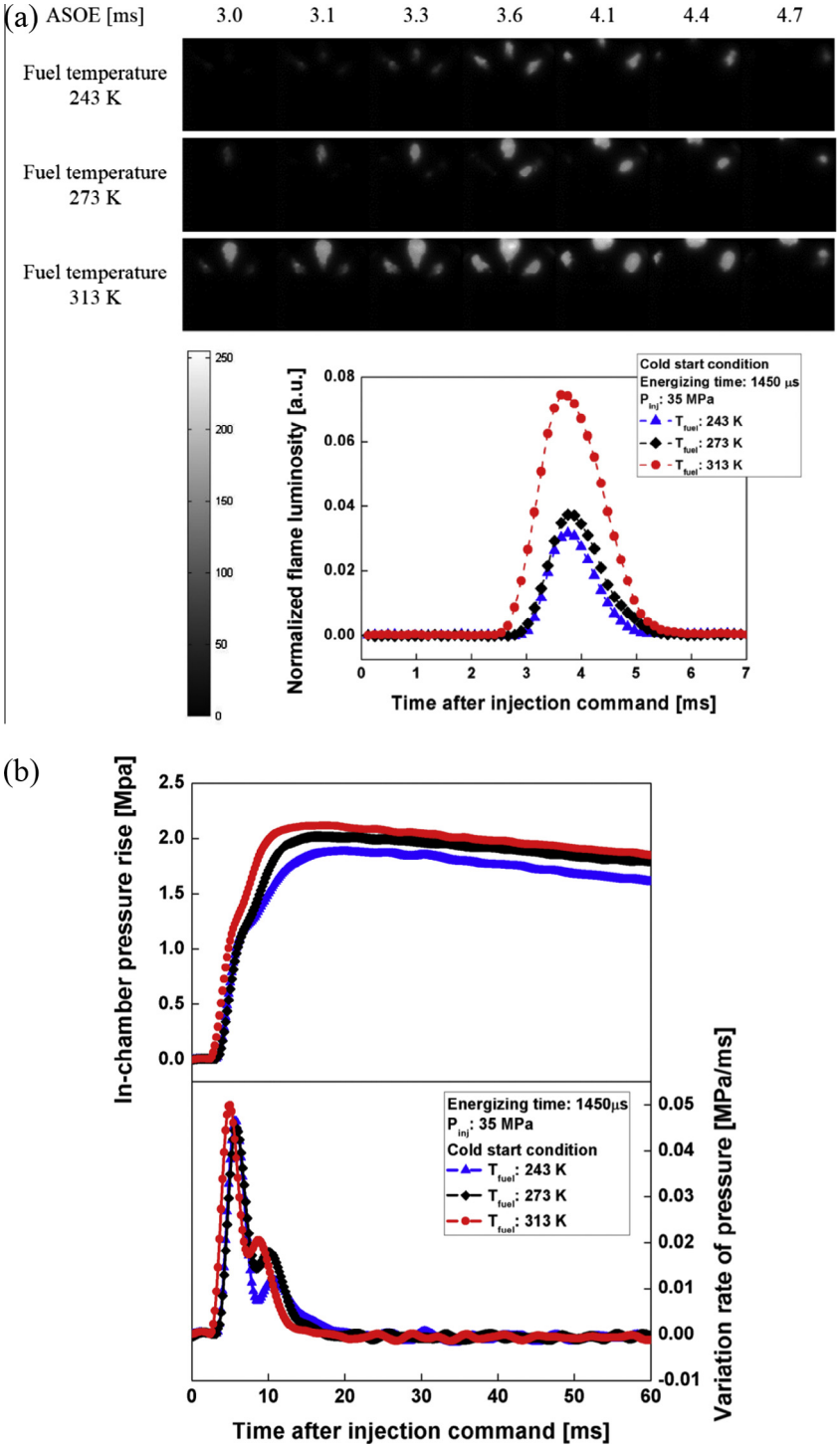

Fig. 8. (a) Normalized flame luminosity, (b) in-chamber pressure rise, and variation of pressure according to fuel temperature under cold start condition.

surface tension [19]. Thus, the cold fuel showed a longer liquid penetration tip length than the warm fuel due to attenuated atomization and vaporization characteristics.

3.2. Effects of ambient condition on combustion

Fig. 7 shows the combustion images, in-chamber pressure rise and variation rate of pressure according to atmospheric conditions. The color bar on the left side indicates the intensity of the natural luminosity. The luminosity intensity was averaged over the combustion chamber. As shown in the Fig. 7(a), only three spray plumes were ignited in the cold start condition while all spray plumes were ignited in a warm up condition. The misfire in the cold start condition is known to be a main factor for the high hydrocarbon emissions and the cycle-to-cycle dispersion [20]. The flame luminosity in the cold start condition appeared at a later time than that of the warm up condition. This indicates that the ignition delay during the cold start condition was longer than that during the hot start condition. This is because of poor mixture preparation caused by attenuated spray atomization and

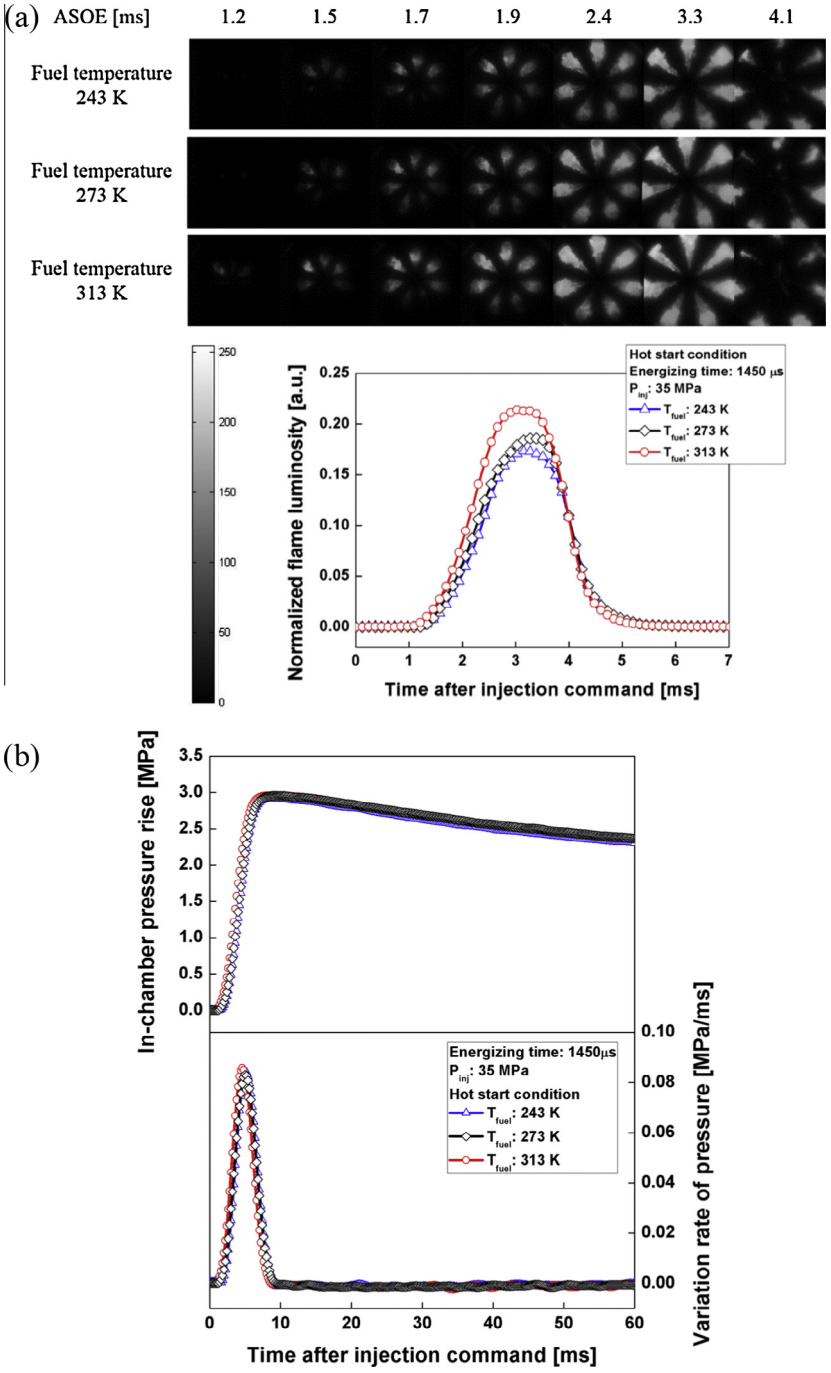

Fig. 9. (a) Normalized flame luminosity, (b) in-chamber pressure rise, and variation of pressure according to fuel temperature under warm up condition.

vaporization. The captured images revealed the flame luminosity to be further away from the nozzle tip and closer to the chamber wall in the cold start condition. This implies that the flame lift of length (LOL) increased as fuel temperature decreased. From the image, the LOL was obtained by measuring the distance from the injector tip to nearest axial location of flame with an intensity greater than the set threshold of 10 on a zero to 255 intensity scale of the image. The LOL of each conditions were measured at 3.6 ms after start of the energizing. The LOL of cold start condition was 2.5 cm whereas, the value of hot start condition was 1.4 cm. From the measurement, the LOL of cold start condition was 1.78 times that of hot start condition. This result is consistent with previous studies that the lift-off length got shortened as the ambient temperature increased [21–23]. Theoretically, the LOL was proposed by Payri to be represented by following equation [24]:

$$\mathrm{LOL} = T_{amb}^{-3.97} \cdot \rho_{amb}^{-0.93} \cdot u_{eff}^{0.52} \cdot T_f^{-0.32} \tag{8}$$

where T_{amb} is the ambient temperature, ρ_{amb} is the ambient density, u_{eff} is the effective velocity at the exit of the orifice, and T_f is the fuel temperature. The fuel temperature is identical and the difference in the effective velocity is negligible for both conditions. Therefore, the LOL can be simplified as a function of the ambient temperature and the density. From the equation, the ratio of LOL $\frac{\mathrm{LOL}_{cold}}{\mathrm{LOL}_{warm-up}}$ was calculated as 1.7, which implies that the LOL of the cold start condition is 1.7 times longer than that of the warm-up condition. This is

associated with the poor mixing and evaporation characteristics in the cold start condition. The peak of the flame luminosity was calculated to be 0.032 for the cold start condition and 0.173 for the warm up condition. In addition, the duration of the visible flame was longer under the hot start condition. The visible flame durations were 4.4 ms and 1.9 ms for hot start and cold start condition respectively. This suggests that the combustion during the hot start condition was more vigorous than that in the cold start condition. On the other hand, the rise in the pressure due to spray flame in the cold start condition was lower than that of the hot start condition. Fig. 7(b) shows that the peak values of the pressure rise were 0.19 and 0.29 MPa for cold and hot start conditions respectively. According to the pressure variation rate, the combustion in hot start condition is noted to have abruptly occurred with a premixed dominant combustion while a diffusion-like phase existed in cold start condition. The reason for this is that the air–fuel mixture preparation during the ignition delay was deteriorated by the lower ambient pressure and the temperature in the cold start condition.

3.3. Effects of fuel temperature on combustion

The combustion image, in-chamber pressure rise and variation rate of the pressure according to fuel temperature are shown in Fig. 8. The three fuel temperature case (243, 273, and 313 K) were compared. Fig. 8(a) shows that partial misfires occurred over the entire fuel temperature range in the cold start condition. The peak of the flame luminosity was calculated to be of 0.032, 0.037, and 0.074 for the fuel temperature of 243, 273, and 313 K, respectively. The start of the combustion was advanced and the duration of the visible flame luminosity was lengthened as the fuel temperature increased. These results imply that combustion with a high temperature fuel was activated by the enhanced fuel atomization characteristics. The longer ignition delay and the deterioration in the combustion can also be seen in results of the in-chamber pressure rise. Fig. 8(b) shows that the peak values of the pressure rise were 0.19, 0.2, and 0.21 MPa for the fuel temperature of 243, 273, and 313 K since the air–fuel mixture preparation with the warm fuel was more advantageous for combustion as confirmed by the spray experiment.

The sequential flame image, the in-chamber pressure rise and the variation rate of the pressure for the hot start condition are shown in Fig. 9. In a similar manner to the cold condition, the ignition delay increased as the fuel temperature decreased as shown in Fig. 9(a). However, the differences of the ignition delay were reduced for the warm-up condition, indicating that the increase in the ambient pressure and the temperature were more dominant factors to improve combustion. Therefore, all spray plumes can be seen to have ignited without a misfire. The peak of the lame luminosity was calculated to be of 0.17, 0.19, and 0.21 for a fuel temperature of 243, 273, and 313 K, respectively. From Fig. 9(b), peak values of the pressure rise were of 0.19, 0.2, and 0.21 MPa for a fuel temperature of 243, 273, and 313 K cases. These values indicate that combustion was facilitated by the elevation in the in-chamber pressure and temperature. The peak of in-chamber pressure variation mainly depends on the combustion rate in the first stage, which is influenced by the fuel taking part in the premixed combustion phase [26]. The premixed combustion phase is becoming dominant as evaporation and atomization characteristics are enhanced. Therefore, the pressure variation rate in hot start condition showed single high peak but the combustion in cold start condition had double peaks as we seen in Figs. 9(b) and 8(b).

4. Conclusion

The effects of the diesel fuel temperature on the spray and combustion characteristics were investigated to provide insight into improving the cold startability of the diesel engines by using a common-rail system and a CVCC. The evaporating spray and the combustion behaviors were observed under various fuel temperature and ambient conditions. The major findings of this study are summarized as follows:

(1) Cold diesel fuel exhibited a longer injection delay than warm diesel fuel due to its higher dynamic viscosity. However, the cold diesel fuel eventually had a longer liquid tip penetration length and a narrower spray angle than the warm diesel fuel, which was attributed to the poor atomization and the vaporization characteristics due to the higher density and viscosity.
(2) The flame luminosity and the peak of the pressure rise decreased for the cold start condition. This implies that the combustion was hindered by the deterioration in the spray characteristics due to the low ambient pressure and temperature. While all spray plumes were ignited in the hot start condition, a partial misfire was confirmed in the cold start condition. The flame lift off length for the cold condition was significantly longer than the hot case.
(3) Combustion was facilitated with the warm fuel showing a higher flame luminosity, peak of pressure rise, and a shorter ignition delay as a result of the enhanced atomization and evaporation characteristics of the high temperature fuel. However, the effects of the fuel temperature were less dominant than those of the ambient condition.
(4) The spray and combustion imaging provided distinct insight into the cold start combustion process. The results suggest that a specific injection strategy, such as with a multiple injection and a higher injection pressure, can promote the air–fuel mixing process and should be applied to improve cold startability.

Acknowledgement

The authors would like to appreciate Hyundai Motor Company for financial and technical support.

References

[1] Henein N, Zahdeh A, Yassine M, Bryzik W. Diesel engine cold starting: combustion instability. SAE Paper 920005; 1992.
[2] Weilenmann M, Jean-Yves Favez, Alvarez R. Cold-start emissions of modern passenger cars at different low ambient temperatures and their evolution over vehicle legislation categories. Atmos Environ 2009;43:2419–29.
[3] Mendez S, Thirouard B. Using multiple injection strategies in diesel combustion: potential to improve emissions, noise and fuel economy trade-off in low CR engines. SAE Trans J Fuels Lubr 2009;1(1):662–74.
[4] Pacaud P, Perrin H, Laget O. Cold start on diesel engine: is low compression ratio compatible with cold start requirements? SAE Trans J Eng 2009;1 (1):831–49.
[5] MacMillan D, La Rocca A, Shayler P, Murphy M, Pegg I. The effect of reducing compression ratio on the work output and heat release characteristics of a DI diesel under cold start conditions. SAE Trans J Eng 2009;1(1):794–803.
[6] Fasolo B, Doisy A, Dupont A, Lavoisier F. Combustion system optimization of a new 2 liter diesel engine For euro IV. SAE Paper 2005-01-0652;2005.
[7] Lindl B, Schmitz Heinz-Georg. Cold-start equipment for diesel direct-injectionengines. SAE Paper 1999-01-1244; 1999.
[8] Payri F, Broatch A, Serrano JR, Rodriguez LF, Esmoris A. Study of the potential of intake air heating in automotive DI diesel engines. SAE Paper 2006-01-1233; 2006.
[9] Broatch A, Ruiz S, Margot X, Gil A. Methodology to estimate the threshold in-cylinder temperature for self-ignition of fuel during cold start of diesel engine. Energy 2010;35(5):2251–60.
[10] Chartier C, Aronsson U, Andersson O, Egnell R. Effect of injection strategy on cold start performance in an optical light-duty DI diesel engine. SAE Paper 2009-09-13; 2009.
[11] Zhong L, Gruenewald S, Henein NA, Bryzik W. Lower temperature limits for cold starting of diesel engine with a common rail fuel injection system. SAE Paper 2007-01-0934; 2007.

[12] Payri R, Salvador FJ, Gimeno J, Bracho G. Understanding diesel injection characteristics in winter conditions. SAE Paper 2009-01-0836; 2009.
[13] Park SH, Kim HJ, Suh HK, Lee CS. Experimental and numerical analysis of spray-atomization characteristics of biodiesel fuel in various fuel and ambient temperatures conditions. Int J Heat Fluid Flow 2009;30(5):960–70.
[14] Kyriakides N, Chryssakis C, Kaiktsis L. Influence of heavy fuel properties on spray atomization for marine diesel engine applications. SAE Paper 2009-01-1858; 2009.
[15] Fox RW, McDonald AT, Pritchard PJ, Leylegian JC. Fluid Mechanics. 8th ed.; 2012.
[16] Bruce RM, Donald FY, Theodore HO. Fundamentals of fluid mechanics. 4th ed. John Wiley & Sons Inc; 2002.
[17] Siebers DL. Liquid-phase fuel penetration in diesel sprays. SAE paper 980809; 1998.
[18] Shoba TT, Crua C, Heikal MR, Gold M. Optical characterization of diesel, RME and kerosene sprays by microscopic imaging. Estoril, Portugal: ILASS-Europe 2011; 2011.
[19] Davanlou A, Lee J, Basu S, Kumar R. Effect of viscosity and surface tension on breakup and coalescence of bicomponent sprays. Chem Eng Sci 2015;131(28):243–55.
[20] Pastor JV, Garcia-Oliver JM, Pastor JM, Ramirez-Hernandez JG. Ignition and combustion development of high speed direct injection diesel engines under low temperature cold start conditions. Fuel 2011;90(4):1556–66.
[21] Siebers DL, Higgins B. Flame lift-off on direct-injection diesel sprays under quiescent conditions. SAE paper 2001-01-0530; 2001.
[22] Higgins BS, Diebers DL. Measurement of the flame lift-off location on DI diesel spray using OH chemiluminescence. SAE paper 2001-01-0918.
[23] Pickett LM, Siebers DL. Soot in diesel fuel jets: effects of ambient temperature, ambient density, and injection pressure. Combust Flame 2004;138(1–2):114–35.
[24] Payri R, Garcia-Oliver JM, Bardi M, Manin J. Fuel temperature influence on diesel sprays in inert and reacting conditions. Appl Therm Eng 2012;35:185–95.
[25] Park Y, Hwang J, Bae C, Kim K, Pyo S, Lee J. Effects of diesel fuel temperature on fuel flow and spray characteristics. Fuel (in preparation).
[26] Kegl B, Hribernik A. Experimental analysis of injection characteristics using biodiesel fuel. Energy Fuels 2006;20:2239–48.